

MEMS-Based Miniature Optical Pickup

Yi Chiu, *Member, IEEE*, Cheng-Huan Chen, Jin-Chern Chiou, Weileun Fang, and Han-Ping D. Shieh, *Senior Member, IEEE*

Abstract—The technology challenges for miniature optical pickups include high-numerical-aperture objective lens design, servo actuator functions and performance, and component assembly tolerance. In this paper, a microelectromechanical systems (MEMS)-based miniature optical pickup is proposed for DVD and blue disk systems. A high-order diffractive objective lens with a continuous surface relief is designed. Focus, tilt, and tracking servos are implanted with MEMS micro actuators. Preliminary design and test results are presented.

Index Terms—Diffractive optical element, microelectromechanical system (MEMS), micromirror, optical pickup.

I. INTRODUCTION

TRADITIONAL optical pickups are composed of discrete optical and mechanical components. Various techniques have been proposed to reduce the weight and volume and simplify the assembly processes. However, devices based on integrated optics [1] suffer from low optical efficiency and focused spot quality due to waveguide coupling. Devices based on stacking [2] are challenged with complicated assembly processes. Recently, microelectromechanical systems (MEMS) technology has been employed to make various electromechanical components for fine servo controls for data storage systems. Wu *et al.* demonstrated a pickup unit based on the free-space microoptical bench technology [3]. Since light propagates in free space in this platform, power loss and aberration due to waveguides can be reduced. The entire optical system on the chip can be fabricated using the microfabrication batch processes. The assembly of various components can also be simplified. Furthermore, it is possible to integrate control and signal processing circuits on the chip to enhance its functions and performance. Therefore, the proposed miniature pickup is based on the free-space microoptical bench technology, as shown schematically in Fig. 1.

The optical system of the proposed module is similar to the traditional optical pickups. Light is delivered to the module by

Manuscript received September 6, 2004. This work was supported in part by the Ministry of Economic Affairs, Taiwan, R.O.C., under Contract 91-EC-17-A-07-S1-0011, by the National Science Council, Taiwan, R.O.C., under Contract 92-2215-E-009-009, and by the Brain Research Center, University System of Taiwan, under Grant 91B-711 and 92B-711.

Y. Chiu and J.-C. Chiou are with the Department of Electrical and Control Engineering, National Chiao Tung University, Hsin Chu 300, Taiwan, R.O.C. (e-mail: yichiu@mail.nctu.edu.tw; chiou@cc.nctu.edu.tw).

C.-H. Chen is with the Department of Electronic Engineering, National Taiwan University of Science and Technology, Taipei, Taiwan, R.O.C. (e-mail: chchen@et.ntust.edu.tw).

W. Fang is with the Department of Power Mechanical Engineering, National Tsing Hua University, Hsin Chu 300, Taiwan, R.O.C. (e-mail: fang@pme.nctu.edu.tw).

H.-P. D. Shieh is with the Institute of Electro-Optical Engineering, National Chiao Tung University, Hsin Chu 300, Taiwan, R.O.C. (e-mail: hpshieh@cc.nctu.edu.tw).

Digital Object Identifier 10.1109/TMAG.2004.842077

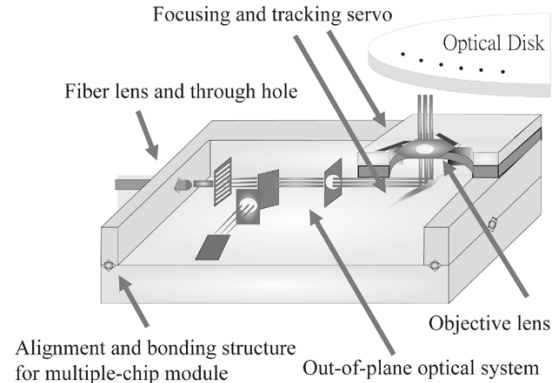


Fig. 1. Schematic of the MEMS-based optical pickup head.

an optical fiber with a micro lens on its end [4]. The laser diode module can then be separated from the pickup module to reduce the weight of moving mass. As a first demonstration, the three-beam tracking method will be used. Collimation, diffraction grating, and beam-splitting components are fabricated with standard surface micromachining technology. A MEMS torsion micromirror is used as the tracking servo. The focusing servo, which is a surface micromachined actuator moving in the vertical direction, is fabricated in another chip. Electrostatic actuation is chosen due to its low power consumption and compatibility of materials and control mechanism. On top of the actuator, the objective lens is made of thick polymer materials such as AZ 4620 or SU-8. The two chips, as well as other alignment and spacing structures, are bonded together with flip-chip bonding technology.

II. OPTICAL DESIGN

Fresnel lens has long been used as an alternative for very-large-size refractive lens to reduce the system size and weight. Pure diffractive or compound refractive-diffractive optical components were also investigated for optical storage applications [5]–[7]. In addition, the photolithography process for semiconductor device fabrication has been successfully used in making binary-type kinoform diffractive element. Therefore, an all-diffractive-type optical system is proposed for the micro pickup.

As shown in Fig. 1, there are three main optical components controlling the laser beam properties and the optical path, namely the collimator, beam splitter, and objective lens. The beam splitter is traditionally a binary grating, whose function cannot be realized with a refractive element. Its efficiency can be improved with a more sophisticated profile and more than one phase step. It was shown that an equal-sided triangular grating with quantized phase steps can achieve an overall efficiency more than 96% for the desired intensity ratio of 10:1 between the central beam and the side beams.

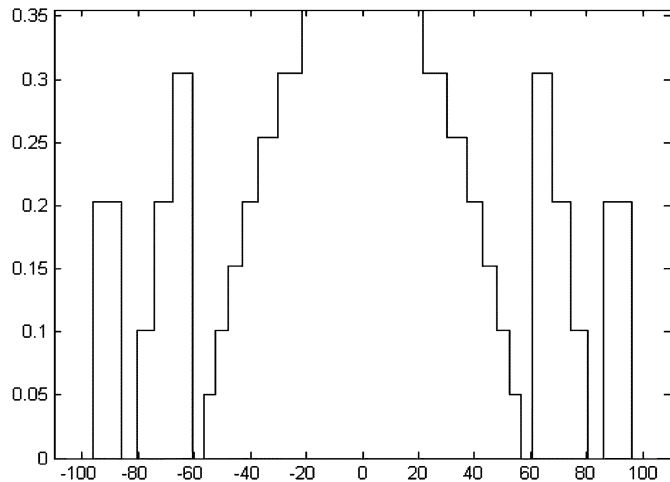


Fig. 2. Staircase-type Fresnel lens with varied phase step for collimator.

The collimation lens can be implemented with a staircase-type Fresnel lens with varied step numbers in accordance to the linewidth limitation of the photolithography process, especially for the peripheral region of the lens. Fig. 2 shows a lens designed with this concept, which still possesses an efficiency of 93% assuming a Gaussian distribution of intensity profile. Both the collimator and the beam splitter can be integrated on a microoptical bench using the same manufacturing process.

The objective lens requests a high optical quality as it determines the size of the focal spot, hence the storage density. The efficiency loss of a staircase-type pure diffractive element will cause deterioration of focal-spot quality. Therefore, a continuous surface relief is essential. A high-order diffractive objective lens with a continuous surface relief in each zone is proposed so that the efficiency will be theoretically 100%. The thickness is chosen in accordance with the process limitation of photolithography, as well as the constructive interference of diffracted light from all zones. Different from the traditional design process of multiorder diffractive lens, the surface profile of each zone is optimized separately for correcting geometrical aberration and then combined together as a compound objective lens. This approach led to an objective lens with a numerical aperture (NA) of $NA = 0.6$, a minimum zone width associated with the outmost zone of $16 \mu\text{m}$, and a focal spot of $1 \mu\text{m}$. The size and weight are nearly one third of its refractive counterpart. The spot profile, based on the simulation using the Advanced System Analysis Program (ASAP) with consideration of the diffraction behavior, is shown in Fig. 3. The coma aberration due to the wobbling of the disk with respect to the lens and the dispersion of diffractive elements are important issues and will be addressed in future development. As the multiorder diffractive lens has its aberration corrected zone by zone, the coma is expected to be lower than that of a pure refractive one. The dispersion of the multiorder diffractive lens will not be as strong as a pure diffractive one, as its refractive behavior still takes quite a weighting. Yet, both issues are subject to investigation.

The continuous surface relief can be fabricated in thick photoresist such as AZ 4620 using gray-scale photomasks such as HEBS [8] or films [9]. The development characteristics curve of the photoresist AZ4620 is shown in Fig. 4. With this characteristics curve, the photomask is currently being designed.

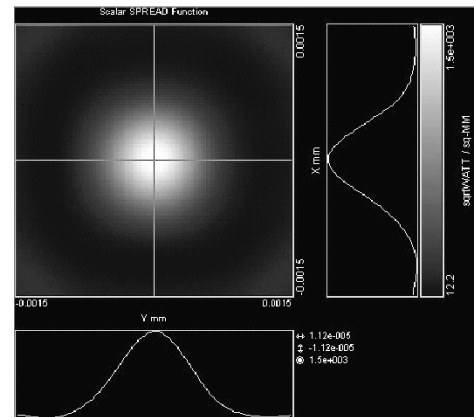


Fig. 3. Diffractive focal spot of the proposed objective.

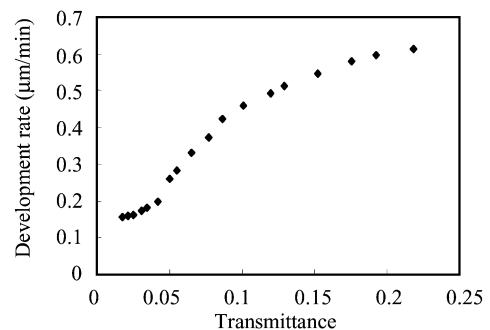


Fig. 4. Development characteristics curve of AZ 4620.

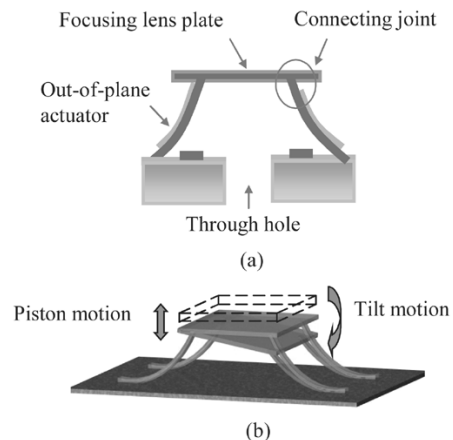


Fig. 5. Microfocusing stage design concept for the optical pickup head (a) components and (b) piston and tilt motions.

III. FOCUSING ACTUATOR

Presently, various micromachined actuators have been employed to tune the tracking and focusing of the light beam of optical pickup heads [10], [11]. This paper demonstrates a novel microfocusing stage. As shown in Fig. 5(a), the microfocusing stage consists of four parts: an out-of-plane actuator, a connecting joint, a through hole, and a focusing lens plate. Stress-induced beams act as the self-assembly mechanism to lift up the focusing lens plate, as well as the out-of-plane electrostatic actuator, after an electrode layer is deposited. Unlike the design in [12], a through hole underneath the lens plate is allowed in this case for the incident light beam. The position of the focusing plate can be controlled by the stress-induced beams, as shown

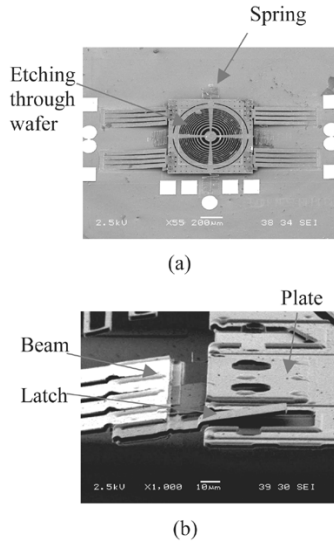


Fig. 6. (a) Microfocusing stage and (b) close-up of the sliding latch.

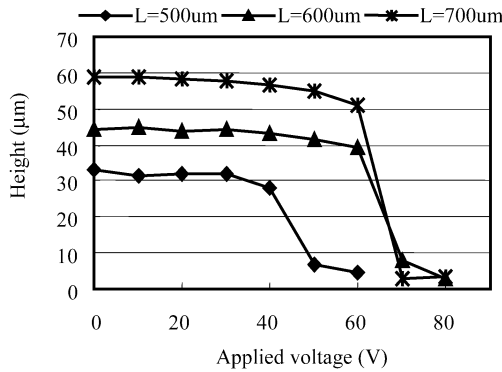


Fig. 7. Tip height of the stress beams with various beam length L .

in Fig. 5(b). The stage has a piston motion to adjust the focal point of the lens. Moreover, it has a tilt motion, which can be used to compensate the disk tilt errors.

The device is realized by a multiuser MEMS processes (MUMPs)-like backside-etching process [13]. The fabricated microfocusing stage is shown in Fig. 6. The lens plate was lifted up for $23 \mu\text{m}$ by the stress-induced beams. The black region in Fig. 6(a) shows the backside-etched through hole. There are four springs on each side of the lens plate. These springs were used to anchor the lens plate on the substrate. Moreover, the restoring force of the spring ensured the contact between the lens plate and latch so that the backlash was prevented [Fig. 6(b)].

Fig. 7 shows the tip height of the stress beams versus the driving voltage with three different beam lengths. The tilt angle was also measured. Typical tilt angles ranged between 1° and 2° . By actuating different beams, the lens on top can be tilted to compensate the relative tilt between the lens and the disk due to disk rotation. The frequency response of this actuator showed a flat response up to several kilohertz, which is much larger than the traditional actuators. However, the stroke of the current micro actuator is only several tens of micrometers. For real applications, where the focusing servo should have a stroke of about 1 mm, a two-stage system combining the MEMS device and a traditional actuator is necessary. In this case, the traditional actuator is used for low-speed coarse focusing, and the

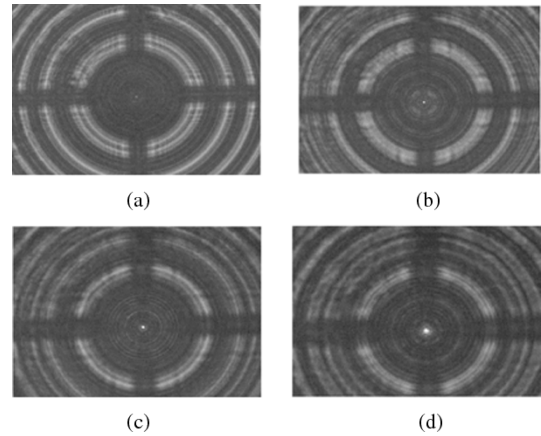


Fig. 8. Spot image at the distance: (a) and (b) shorter than focal length, (c) equal to focal length, and (d) longer than focal length.

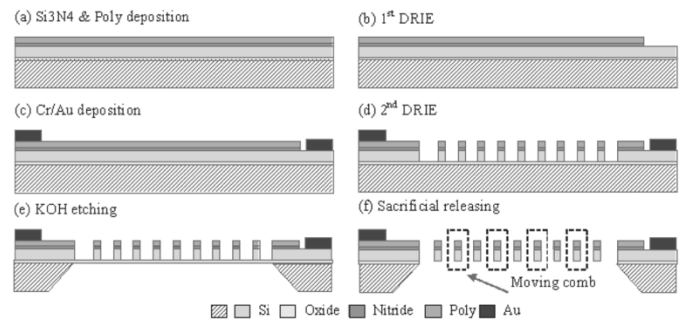


Fig. 9. Process flow of the microscanning mirror.

MEMS actuator is used for high-speed fine focusing and tilt compensation.

A binary amplitude-type Fresnel lens was fabricated to demonstrate the focusing function of this microstage. The zone plate was fabricated using polysilicon and standard photolithography due to their readiness for process integration. A 650-nm laser beam was incident on the Fresnel lens from the backside of the substrate and then focused on a microscope objective lens. Thus, the spot size of the focusing beam and the associated focusing depth were measured, as shown in Fig. 8. A typical measured spot size was $4.8 \mu\text{m}$ at $1/e^2$, and focal depth was $1054 \mu\text{m}$. The focused spot size of this binary lens is far from optimized; a better designed phase-type lens, as discussed previously, is being fabricated.

IV. TRACKING ACTUATOR

The MEMS-based electrostatic torsion micromirror has been widely studied [14]–[16]. The main design issues for torsion micromirrors include reflective area size, flatness, rotation angle, driving voltage, resonant frequency, and bandwidth. In this study, a scanning micromirror made in a silicon-on-insulator (SOI) substrate was used as the tracking actuator due to the flat reflecting surface and thicker and more rigid mechanical structure. The process flow of the proposed SOI vertical comb-drive micromirror is shown in Fig. 9. The vertical comb consists of a stack of the deposited polysilicon layer as the upper electrode, an insulation layer, and the device layer of the SOI substrate as the lower electrode. The comb structure

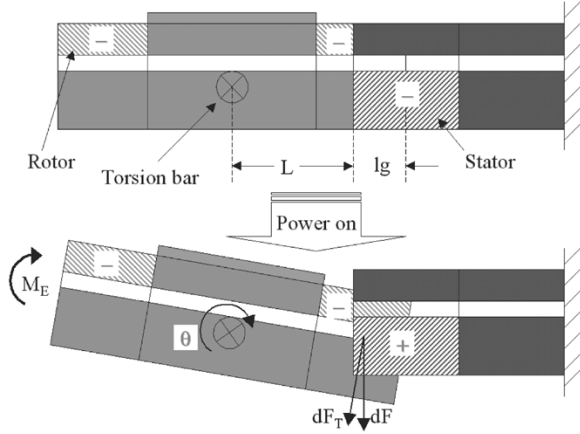


Fig. 10. Mechanical model of the rotation micromirror.

is defined by inductively coupled plasma reactive ion etching (ICP RIE) processes and released by wet etching.

For mechanical analysis, the cross section of the vertical comb drive is illustrated in Fig. 10, where L is a constant distance between the rotation axial and the comb finger tip, and lg is the length of active comb finger. When a bias voltage is applied to the rotor and stator fingers, the induced electrostatic force dF produces a moment M_E to the micromirror. In static analysis, the following equation holds:

$$M_E(\theta, V) = T\theta \quad (1)$$

where T is the torsion constant, θ is the rotation angle, V is the driving voltage, and M_E is a function of V and θ . For a single pair of the comb drive, the moment m_E applied by the comb drive can be expressed as

$$m_E = \int_{\ell=0}^{\ell=lg} F(z) \cdot \cos \theta \cdot (L + \ell) \cdot V^2 \cdot d\ell \quad (2)$$

where $F(z)$ is the unit electrostatic function that can be obtained from two-dimensional (2-D) simulation of single-pair comb drive [17]. Since there are N fingers in a set of stators, the overall moment M_E can be rewritten as

$$\begin{aligned} M_E(\theta, V) &= N \cdot \int_{\ell=0}^{\ell=lg} F(z) \cdot \cos \theta \cdot (L + \ell) \cdot V^2 \cdot d\ell \\ &= N \cdot V^2 \cdot \cos \theta \cdot \int_{\ell=0}^{\ell=lg} F(z) \cdot (L + \ell) \cdot d\ell. \end{aligned} \quad (3)$$

By using (1) and (3), the relation between rotation angle and bias voltage can be obtained. Note that with 200-V bias voltage and 0.1-V resolution, $\pm 0.96^\circ$ maximum rotation angles (θ_M) and 0.00048° rotation resolution can be achieved. In the present design, upon the application of a coarse tuning bias voltage, a voltage of 0.1 V is further applied to the fine-tuning stators [16], which can reach a maximum fine-tuning rotation angle of

$1.65 \times 10^{-6}^\circ$ according to simulation. This will greatly enhance the rotation resolution.

V. CONCLUSION

A miniature optical pickup based on surface micromachining, SOI micromachining, deep reactive ion etching, and flip-chip bonding is proposed. Electrostatic MEMS actuators are used for focusing and tracking servo actuators. A 0.6-NA harmonic diffractive objective lens was designed with a spot size approaching the diffraction limit. A microfocusing stage is demonstrated. Further fabrication and testing are in progress.

REFERENCES

- [1] S. Ura, T. Suhara, H. Nishihara, and J. Koyama, "An integrated-optic disc pickup device," *Electronics Communications in Japan, Part 2: Electronics (English Transl. Denshi Tsushin Gakkai Ronbunshi)*, vol. 70, no. 2, pp. 92–100, 1987.
- [2] S. Yoshida, M. Ogawa, T. Saeki, Y. Sekimoto, Y. Kurata, and Z. Tani, "MD optical pickup integrated with a birefringence wedge and an HOE," in *Dig. Internal Symp. Optical Memory (ISOM 2001)*, 2002, pp. 126–127.
- [3] M. Wu, "Micromachining for optical and optoelectronic systems," *Proc. IEEE*, vol. 85, no. 11, pp. 1833–1856, Nov. 1997.
- [4] C.-H. Tien, T. Milster, Y. Chiu, and H.-P. D. Shieh, "Design and fabrication of fiberlenses for optical recording applications," *Jpn. J. Appl. Phys.*, vol. 41, no. 3B, pp. 1834–1837, 2002.
- [5] K. Goto, Y. Higuchi, and K. Mori, "Plastic grating collimating lens," *Proc. SPIE*, vol. 1139, pp. 169–176, 1989.
- [6] K. Goto, K. Mori, G. Hatakoshi, and S. Takahashi, "Spherical grating objective lenses for optical disk pick-ups," *Jpn. J. Appl. Phys.*, vol. 26, no. 4, pp. 135–140, 1987.
- [7] K. Goto and K. Mori, "Design of aberration free spherical microlens with a diffractive relief grating film on a refractive spherical glass substrate," *Jpn. J. Appl. Phys.*, vol. 31, no. 5B, pp. 1586–1590, 1992.
- [8] W. Daschner, P. Long, R. Stein, C. Wu, and S. H. Lee, "Cost-effective mass fabrication of multilevel optical elements by use of a single optical exposure with a gray-scale mask on high-energy beam-sensitive glass," *Appl. Opt.*, vol. 36, no. 20, pp. 4675–4680, 1997.
- [9] T. J. Suleski and D. C. O'Shea, "Gray-scale masks for diffractive-optics fabrication: I commercial slide imagers," *Appl. Opt.*, vol. 34, no. 32, pp. 7507–7517, 1995.
- [10] L. Fan, M. C. Wu, K. D. Choquette, and M. H. Crawford, "Self-assembled microactuated XYZ stages for optical scanning and alignment," in *Dig. Int. Conf. Solid-State Sensors, Actuators, Microsystems (Transducers)*, 1997, pp. 319–322.
- [11] I. Watanabe, Y. Ikai, T. Kawabe, H. Kobayashi, S. Ueda, and J. Ichihara, "Precise track-following control using a MEMS tracking mirror in high-density optical disk drives," in *Dig. Joint Internal Symp. Optical Memory Optical Data Storage (ISOM/ODS 2002)*, 2002, pp. 257–259.
- [12] M. A. Helmbrecht, U. Srinivasan, C. Rembe, R. T. Howe, and R. S. Muller, "Micromirrors for adaptive-optics arrays," in *Dig. Int. Conf. Solid-State Sensors, Actuators, Microsystems (Transducers)*, 2001, pp. 1290–1293.
- [13] H.-Y. Lin, "The hybrid micromachined silicon-optical-bench and its applications," Ph.D. dissertation, Power Mechanical Engineering Dept., National Tsing-Hwa Univ., Taiwan, R.O.C., 2002.
- [14] Z. Hao, B. Wingfield, M. Whitley, J. Brooks, and J. A. Hammer, "A design methodology for a bulk-micromachined two-dimensional electrostatic torsion micromirror," *J. Microelectromech. Syst.*, vol. 12, pp. 692–701, 2003.
- [15] U. Krishnamoorthy, D. Lee, and O. Solgaard, "Self-aligned vertical electrostatic combdrives for micromirror actuation," *J. Microelectromech. Syst.*, vol. 12, pp. 458–464, 2003.
- [16] J. C. Chiou and Y. C. Lin, "A multiple electrostatic electrodes torsion micromirror device with linear stepping angle effect," *J. Microelectromech. Syst.*, vol. 12, pp. 913–920, 2003.
- [17] J. C. Chiou and Y. J. Lin, "A new modeling method of vertical electrostatic comb drive," *Int. J. Computat. Eng. Sci.*, vol. 4, no. 3, pp. 641–644, 2003.